Smart Structures and Systems, *Vol. 22, No. 3 (2018) 327-334*
DOI: https://doi.org/10.12989/sss.2018.22.3.327

Dynamic buckling of smart sandwich beam subjected to electric field based on hyperbolic piezoelasticity theory

Maryam Shokravi*

Buein Zahra Technical University, Buein Zahra, Qazvin, Iran

(Received May 2, 2018, Revised July 8, 2018, Accepted July 10, 2018)

Abstract. In this paper, dynamic buckling of the smart subjected to blast load subjected to electric field is studied. The sandwich structure is rested on Pasternak foundation with springs and shear elements. Applying piezoelasticity theory and hyperbolic shear deformation beam theory (HSDBT), the motion equations are derived by energy method. For calculating the dynamic instability region (DIR) of the sandwich structure, differential quadrature method (DQM) along with Bolotin method is used. The aim of this study is to investigate the effects of applied voltage, geometrical parameters of structure and boundary conditions on the DIR of the structure. The results show that applying negative voltage, the DIR will be happened at higher excitation frequencies. In addition, the clamped-clamped beam leads to higher excitation frequency with respect to simply supported boundary condition.

Keywords: dynamic buckling; electric field; HSDBT; DQM; piezoelasticity theory

1. Introduction

Sandwich structures can be used in different industries such as aerospace, aircraft, automobile and etc due to high strength and low weight with respect to traditional materials. One of the important ways for control of the sandwich structures, is using piezoelectric materials since in these materials, the structure subjected to mechanical forces can produces the electric field and vice versa (Yang and Yu 2017, Henderson *et al*. 2018, Ghini and Vacca 2018).

Dynamic analysis of sandwich structures has been reported by researchers. An investigation on the nonlinear dynamic response and vibration of the imperfect laminated three-phase polymer nanocomposite panel resting on elastic foundations was presented by Duc *et al.* (2015). Van Thu and Duc (2016) presented an analytical approach to investigate the non-linear dynamic response and vibration of an imperfect three-phase laminated nanocomposite cylindrical panel resting on elastic foundations in thermal environments.Shokravi and Jalili (2017) studied nonlocal temperature-dependent dynamic buckling analysis of embedded sandwich micro plates reinforced by functionally graded carbon nanotubes. Shokravi (2017a) presented temperature-dependent buckling analysis of sandwich nanocomposite plates resting on elastic medium subjected to magnetic field. Buckling analysis of embedded laminated plates with nanocomposite layers was studied by Shokravi (2017b). Duc *et al.* (2017a, b, c) studied thermal and mechanical stability of a functionally graded composite truncated conical shell, plates and double curved shallow shells reinforced by carbon nanotube fibers. Based on Reddy's third-order shear deformation plate theory, the nonlinear dynamic response and vibration of imperfect functionally graded carbon nanotube-reinforced composite plates was analyzed by Thanh *et al*. (2017). Duc *et al.* (2018) presented the first analytical approach to investigate the nonlinear dynamic response and vibration of imperfect rectangular nanocompsite multilayer organic solar cell subjected to mechanical loads using the classical plate theory. Katariya *et al*. (2017) reported the thermal buckling strength of the sandwich shell panel structure and subsequent improvement of the same by embedding shape memory alloy (SMA) fibre via a general higher-order mathematical model in conjunction with finite element method. The axisymmetric buckling delamination of the Piezoelectric/Metal/Piezoelectric (PZT/Metal/PZT) sandwich circular plate with interface penny-shaped cracks was investigated by Cafarova *et al.* (2017). To control the stochastic vibration of a vibration-sensitive instrument supported on a beam, the beam was designed by Ying *et al.* (2017) as a sandwich structure with magneto-rheological visco-elastomer (MRVE) core. Aerothermoelastic flutter and thermal buckling characteristics of sandwich panels with the pyramidal lattice core resting on elastic foundations in supersonic airflow were studied by Chai *et al.* (2017). A critical review of literature on bending, buckling and free vibration analysis of shear deformable isotropic, laminated composite and sandwich beams based on equivalent single layer theories, layerwise theories, zig-zag theories and exact elasticity solution was presented by Sayyad and Ghugal (2017). Song and Li (2017) investigated the flutter and buckling properties of sandwich panels with triangular lattice core in supersonic airflow, and the active flutter and buckling control are also carried out, which can provide theoretical basis for the use of sandwich structures

*Corresponding author, Ph.D.
E-mail: Maryamshokravi10@bzte.ac.ir

ISSN: 1738-1584 (Print), 1738-1991 (Online)

in the design of aircrafts. Van Do and Lee (2017) reported thermal buckling analyses of functionally graded material (FGM) sandwich plates using an improved mesh-free radial point interpolation method (RPIM). Latifi *et al.* (2018) studied nonlinear dynamic instability analysis of three-layered composite beams with viscoelastic core subjected to combined lateral and axial loadings. Li *et al.* (2018) focused on the post-buckling and free vibration of the sandwich beam theoretically in thermal environments with simply supported and clamped boundary conditions. Shamshuddin Sayyad and Ghugal (2018) investigated the bending, buckling, and vibration responses of shear deformable laminated composite and sandwich beams using trigonometric shear and normal deformation theory. Analytical closed-form solutions for thermos-mechanical stability and explicit expressions for free- and forced-vibration of thin functionally graded sandwich shells with double curvature resting on elastic bases were investigated by Trinh and Kim (2018).

In this paper, dynamic buckling of sandwich beam with piezoelectric layers subjected electric field is studied. The structure is modeled by HSDBT and the motion equations are derived by energy method. The elastic foundation is simulated by Pasternak model with spring and shear elements. The DIR of the structure is calculated by DQM in conjunction with Bolotin method. The effects of applied voltage, geometrical parameters of structure and boundary conditions on the DIR of the structure are shown.

2. Formulation

In Fig. 1, a sandwich beam subjected to electric field is shown. The length of the structure is L and the thickness of core, top and bottom layers are shown by h_c, h_t and h_b, respectively. The structure is rested in Pasternak foundation with spring and shear elements.

2.1 HSDBT theory

There are many new theories for modeling of different structures. Some of the new theories have been used by Tounsi and co-authors (Ait Amar Meziane 2014, Hamidi 2015, Draiche 2016, Attia 2015, Larbi Chaht 2015, Mahi 2015, Ait Yahia 2015, Menasria 2017, Mouffoki 2017, Khetir 2017).

Applying HSDBT, the displacements fields can be written as (Simsek and Reddy 2013)

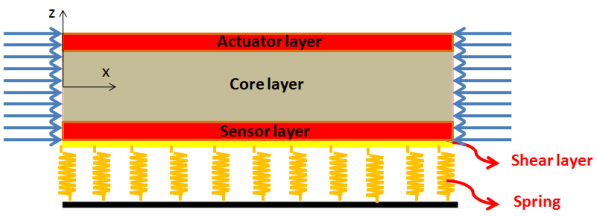

Fig. 1 Schematic of sandwich beam rested in Pasternak foundation

$$\begin{aligned} u_1(x,z,t) &= u(x,t) - z\frac{\partial w(x,t)}{\partial x} \\ &+ \underbrace{\left(h\sinh\left(\frac{z}{h}\right) - z\cosh\left(\frac{1}{2}\right)\right)}_{\Phi(z)}\left(\frac{\partial w(x,t)}{\partial x} - \psi(x,t)\right), \\ u_2(x,z,t) &= 0, \\ u_3(x,z,t) &= w(x,t), \end{aligned} \tag{1}$$

where u and w are the mid-plane displacements in the longitudinal and thickness directions, respectively. Also, ψ denotes the rotation of the cross section area; $h = h_t + h_c + h_b$. However, the strain-displacement relations of the structure are given as below

$$\varepsilon_{xx} = \left(\frac{\partial u}{\partial x}\right) - z\left(\frac{\partial^2 w}{\partial x^2}\right) + \left(h\sinh\left(\frac{z}{h}\right) - z\cosh\left(\frac{1}{2}\right)\right)\left(\frac{\partial^2 w}{\partial x^2} - \frac{\partial \psi}{\partial x}\right), \tag{2}$$

$$\gamma_{xz} = \left(\cosh(z) - \cosh\left(\frac{1}{2}\right)\right)\left(\frac{\partial w}{\partial x} - \psi\right). \tag{3}$$

2.2 Basic relations

The stress-strain relations of the core layer are

$$\sigma_{xx}^{c} = C_{11}\varepsilon_{xx}, \tag{4}$$

$$\tau_{xz}^{c} = C_{44}\gamma_{xz}, \tag{5}$$

where C_{11} and C_{44} are the elastic constants of the core. Also, based on piezoelasticity theory, the constitutive relation of the piezoelectric facesheets can be expressed as (Madani *et al.* 2016)

$$\sigma_{xx}^{p} = Q_{11}\varepsilon_{xx} - e_{31}E_z, \tag{6}$$

$$\tau_{xz}^{p} = Q_{44}\gamma_{xz} - e_{15}E_x, \tag{7}$$

$$D_x = e_{15}\varepsilon_{xz} + \in_{11} E_x, \tag{8}$$

$$D_z = e_{31}\gamma_{xx} + \in_{33} E_z, \tag{9}$$

in which Q_{11} and Q_{44} are the elastic constants; e_{31} and e_{15} are the piezoelectric constants; $\in_{11}$ and $\in_{33}$ are the dielectric constants; D_x and D_z are the electric displacements in the x- and z- directions, respectively; E_x and E_z are the electric fields in the x- and z- directions,

respectively which can be defined as

$$E_k = -\nabla\Gamma \quad \mathrm{k} = \mathrm{x}, \mathrm{z} \tag{10}$$

where Γ is the electric potential which is given for top and bottom layers as

$$\Gamma^t(x,z,t) = -\cos\left(\frac{\pi\left(z - h_c/2\right)}{h_t}\right)\varphi^t(x,t) + \frac{2V_0\left(z - h_c/2\right)}{h_t}, \tag{11}$$

$$\Gamma^b(x,z,t) = -\cos\left(\frac{-\pi\left(z + h_c/2\right)}{h_b}\right)\varphi^b(x,t), \tag{12}$$

where V_0 is the external voltage which is applied to the actuator layer.

2.3 Energy method

The potential strain energy in the structure is given as follows

$$U = \frac{1}{2}\int_V \left(\sigma_{xx}^c \varepsilon_{xx} + \tau_{xz}^c \gamma_{xz}\right)dV + \frac{1}{2}\int_V \left(\sigma_{xx}^p \varepsilon_{xx} + \tau_{xz}^p \varepsilon_{xz} - D_x E_x - D_z E_z\right)dV, \tag{13}$$

By substituting Eqs. (2) and (3) into Eq. (13) we have

$$U = \frac{1}{2}\int_0^L \left[\int \left[N_x\left(\left(\frac{\partial u}{\partial x}\right)\right) - M_x\left(\frac{\partial^2 w}{\partial x^2}\right) + F_x\left(\frac{\partial^2 w}{\partial x^2} - \frac{\partial \psi}{\partial x}\right) + Q_x\left(\left(\frac{\partial w}{\partial x} - \psi\right)\right)\right]dx + \int_V \begin{pmatrix} -D_x\left(\cos\left(\frac{\pi\left(z - h_c/2\right)}{h_t}\right)\frac{\partial \phi^t}{\partial x}\right) \\ -D_z\left(-\frac{\pi}{h}\sin\left(\frac{\pi\left(z - h_c/2\right)}{h_t}\right)\phi^t - \frac{2V_0}{h}\right) \end{pmatrix} dV + \int_V \left(-D_x\left(\cos\left(\frac{-\pi\left(z + h_c/2\right)}{h_b}\right)\frac{\partial \phi^b}{\partial x}\right) - D_z\left(-\frac{\pi}{h}\sin\left(\frac{-\pi}{h_b}\right)\phi^b\right)\right)dV, \tag{14}$$

where the stress resultants are

$$N_x = \int \sigma_{xx}^c dA^c + \int \sigma_{xx}^p dA^p, \tag{15}$$

$$M_x = \int \sigma_{xx}^c z dA^c + \int \sigma_{xx}^p z dA^p, \tag{16}$$

$$F_x = \int \sigma_{xx}^c \Phi(z) dA^c + \int \sigma_{xx}^p \Phi(z) dA^p, \tag{17}$$

$$Q_x = \int \tau_{xz}^c \frac{\partial \Phi(z)}{\partial z} dA^c + \int \tau_{xz}^p \frac{\partial \Phi(z)}{\partial z} dA^p, \tag{18}$$

Substituting Eqs. (3)-(10) into Eqs. (15)-(18), the stress resultants can be calculated as

$$N_x = A_{11}\left(\frac{\partial u}{\partial x} + \frac{1}{2}\left(\frac{\partial w}{\partial x}\right)^2\right) - B_{11}\left(\frac{\partial^2 w}{\partial x^2}\right) + E_{11}\left(\frac{\partial^2 w}{\partial x^2} - \frac{\partial \psi}{\partial x}\right), \tag{19}$$

$$M_x = B_{11}\left(\frac{\partial u}{\partial x} + \frac{1}{2}\left(\frac{\partial w}{\partial x}\right)^2\right) - D_{11}\left(\frac{\partial^2 w}{\partial x^2}\right) + F_{11}\left(\frac{\partial^2 w}{\partial x^2} - \frac{\partial \psi}{\partial x}\right) + \Xi_{31}\phi, \tag{20}$$

$$F_x = E_{11}\left(\frac{\partial u}{\partial x} + \frac{1}{2}\left(\frac{\partial w}{\partial x}\right)^2\right) - F_{11}\left(\frac{\partial^2 w}{\partial x^2}\right) + H_{11}\left(\frac{\partial^2 w}{\partial x^2} - \frac{\partial \psi}{\partial x}\right) + \Im_{31}\phi, \tag{21}$$

$$Q_x = L_{44}\left(\frac{\partial w}{\partial x} - \psi\right) + \Re_{15}\phi, \tag{22}$$

in which

$$A_{11} = \int C_{11} dA^c + \int Q_{11} dA^p, \tag{23}$$

$$B_{11} = \int C_{11} z dA^c + \int Q_{11} z dA^p, \tag{24}$$

$$E_{11} = \int C_{11} \Phi(z) dA^c + \int Q_{11} \Phi(z) dA^p, \tag{25}$$

$$F_{11} = \int C_{11} z\, \Phi(z) dA^c + \int Q_{11} z\, \Phi(z) dA^p, \tag{26}$$

$$H_{11} = \int C_{11} \Phi(z)^2 dA^c + \int Q_{11} \Phi(z)^2 dA^p, \tag{27}$$

$$L_{44}=\int C_{44}\frac{\partial\Phi(z)}{\partial z}dA^{c}+\int Q_{44}\frac{\partial\Phi(z)}{\partial z}dA^{p}. \quad (28)$$

$$\Xi_{31}=\int e_{31}\left(\frac{\pi}{h}\sin\left(\frac{\pi z}{h}\right)\right)dA^{c}, \quad (29)$$

$$\Im_{31}=\int e_{31}\left(\frac{\pi}{h}\sin\left(\frac{\pi z}{h}\right)\right)\Phi(z)dA^{c}, \quad (30)$$

$$\Re_{15}=-\int e_{15}\left(\cos\left(\frac{\pi z}{h}\right)\right)\frac{\partial\Phi(z)}{\partial z}dA^{c}, \quad (31)$$

The kinetic energy of the structure are defined as below

$$K=\frac{\rho}{2}\int\left(\dot{u}_1^{\,2}+\dot{u}_2^{\,2}+\dot{u}_3^{\,2}\right)dV \quad (32)$$

By substituting Eq. (1) into Eq. (32) we have

$$K=\frac{\rho_c+\rho_p}{2}\int\left(\begin{array}{l}\left(\dfrac{\partial u}{\partial t}-z\dfrac{\partial^2 w}{\partial x\,\partial t}\right.\\ \left.+z\left(\dfrac{\partial^2 w}{\partial x\,\partial t}-\dfrac{\partial\psi}{\partial t}\right)\right)^2\\ +\left(\dfrac{\partial w}{\partial t}\right)^2\end{array}\right)dV. \quad (33)$$

where ρ_c and ρ_p are density of core and piezoelectric layers, respectively. By defining the inertia moment terms as

$$\begin{Bmatrix}I_0\\I_1\\I_2\\I_3\\I_4\\I_5\end{Bmatrix}=\int\begin{bmatrix}\rho_c\\\rho_c z\\\rho_c z^{\,2}\\\rho_c\Phi(z)\\\rho_c z\,\Phi(z)\\\rho_c\Phi(z)^2\end{bmatrix}dA^{c}+\int\begin{bmatrix}\rho_p\\\rho_p z\\\rho_p z^{\,2}\\\rho_p\Phi(z)\\\rho_p z\,\Phi(z)\\\rho_p\Phi(z)^2\end{bmatrix}dA^{p}, \quad (34)$$

Eq. (33) can be rewritten as below

$$\begin{aligned}K=0.5\int\Bigg[&I_0\left(\left(\frac{\partial u}{\partial t}\right)^2+\left(\frac{\partial w}{\partial t}\right)^2\right)-2I_1\left(\frac{\partial u}{\partial t}\frac{\partial^2 w}{\partial x\,\partial t}\right)\\&+I_2\left(\frac{\partial^2 w}{\partial x\,\partial t}\right)^2+I_3\frac{\partial u}{\partial t}\left(\frac{\partial^2 w}{\partial x\,\partial t}-\frac{\partial\psi}{\partial t}\right)\\&-I_4\frac{\partial^2 w}{\partial x\,\partial t}\left(\frac{\partial^2 w}{\partial x\,\partial t}-\frac{\partial\psi}{\partial t}\right)+I_5\left(\frac{\partial^2 w}{\partial x\,\partial t}-\frac{\partial\psi}{\partial t}\right)^2\Bigg]dx.\end{aligned} \quad (35)$$

The external work due the Pasternak foundation can be expressed as

$$W_k=-\int(-k_w w+k_g\nabla^2 w)w\,dA, \quad (36)$$

where k_w and k_g are spring constants and shear constants of foundation, respectively.

2.4 Hamilton's principle

Based on Hamilton's principle we have

$$\delta u:\frac{\partial N_x}{\partial x}=I_0\frac{\partial^2 u}{\partial t^2}+(I_3-I_1)\frac{\partial^3 w}{\partial x\,\partial t^2}-I_3\frac{\partial^2\psi}{\partial t^2}, \quad (37)$$

$$\begin{aligned}&\delta w:\frac{\partial^2 M_x}{\partial x^2}+2e_{31}V_0\frac{\partial^2 w}{\partial x^2}-\frac{\partial^2 F_x}{\partial x^2}+\frac{\partial Q_x}{\partial x}\\&-k_w w+k_g\nabla^2 w=I_0\frac{\partial^2 w}{\partial t^2}+(I_1-I_3)\frac{\partial^3 u}{\partial x\,\partial t^2}\\&+(2I_4-I_2-I_5)\frac{\partial^4 w}{\partial x^2\partial t^2}+(I_5-I_4)\frac{\partial^3\psi}{\partial x\,\partial t^2},\end{aligned} \quad (38)$$

$$\delta\psi:Q_x-\frac{\partial F_x}{\partial x}=I_5\frac{\partial^2\psi}{\partial t^2}-I_3\frac{\partial^2 u}{\partial t^2}+(I_4-I_5)\frac{\partial^3 w}{\partial x\,\partial t^2}, \quad (39)$$

$$\delta\phi^{t}:\int_{h_c/2}^{h_c/2+h_t}\left(\begin{array}{l}\dfrac{\partial D_x}{\partial x}\left(\cos\left(\dfrac{\pi(z-h_c/2)}{h_t}\right)\right)\\ D_z\left(-\dfrac{\pi}{h}\sin\left(\dfrac{\pi(z-h_c/2)}{h_t}\right)\right)\end{array}\right)dz=0 \quad (40)$$

$$\delta\phi^{b}:\int_{-h_c/2}^{-h_c/2-h_b}\left(\begin{array}{l}\dfrac{\partial D_x}{\partial x}\left(\cos\left(\dfrac{-\pi(z+h_c/2)}{h_b}\right)\right)\\ +D_z\left(-\dfrac{\pi}{h}\sin\left(\dfrac{-\pi}{h_b}\right)\right)\end{array}\right)dz=0 \quad (41)$$

Substituting Eqs. (19)-(22) into Eqs. (37)-(41), the motion equations of the structure can be derived.

3. Solution procedure

Based on DQ method, we have (Shokravi 2017c)

$$\frac{d^n f(x_i)}{dx^n}=\sum_{j=1}^{N}C_{ij}^{(n)}f(x_j)\qquad n=1,...,N-1. \quad (42)$$

where N denotes number of grid and C_{ij} indicates the weighting coefficients (Hajmohammad, 2018). Finally, the

motion equations can be written in matrix form as

$$\left([K]\begin{Bmatrix}\{d_b\}\\ \{d_d\}\end{Bmatrix}+[C]\begin{Bmatrix}\{\dot{d}_b\}\\ \{\dot{d}_d\}\end{Bmatrix}+[M]\begin{Bmatrix}\{\ddot{d}_b\}\\ \{\ddot{d}_d\}\end{Bmatrix}\right)=\begin{Bmatrix}\{0\}\\ \{0\}\end{Bmatrix}, \quad (43)$$

in which $[K]$, $[C]$ and $[M]$ indicate the stiffness matrix, damper matrix and the mass matrix, respectively. Also, $\{d_b\}$ and $\{d_d\}$ denote boundary and domain points, respectively.

In order to determinate the boundaries of dynamic instability regions, the method suggested by Bolotin is applied. Hence, the components of $\{d\}$ can be written in the Fourier series with period $2T$ as

$$\{d\}=\sum_{k=1,3,\ldots}^{\infty}\left[\{a\}_k \sin\frac{k\omega t}{2}+\{b\}_k \cos\frac{k\omega t}{2}\right], \quad (44)$$

According to this method, the first instability region is usually the most important in studies of structures. It is due to the fact that the first DIR is wider that other DIRs and structural damping in higher regions becomes neutralize. Substituting Eq. (44) into Eq. (43) and setting the coefficients of each sine and cosine as well as the sum of the constant terms to zero, yields

$$\left|\left([K]-P_{cr}\alpha[K]_G\pm P_{cr}\frac{\beta}{2}[K]_G\mp[C]\frac{\omega}{2}-[M]\frac{\omega^2}{4}\right)\right|=0, \quad (45)$$

Solving the above equation based on eigenvalue problem, the variation of ω with respect to α can be plotted as DIR.

4. Numerical results

In this section, the effects of different parameters are shown on the DIR of the sandwich structure. The core of the structure is Polyethylene with Yong' modulus of $E_c=1\,GPa$ integrated with Polyvinylidene Fluoride (PVDF) with Yong' modulus of $E_p=1.1\,GPa$.

The convergence of the proposed method is shown in Fig. 2. It can be found that with rising the grid point numbers of DQ method, the DIR shifts to lower frequencies and finally at N=17, the results become converge.

For comparison the results predicted by hyperbolic theory, the DIR is calculated by Euler theory assuming $\Phi(z)=0$. It can be seen that the DIR predicted by hyperbolic theory is happened at lower excitation frequency with respect to Euler ones. It is since, the flexibility of the hyperbolic theory is higher than Euler ones.

Fig. 4 demonstrates the effect of various boundary conditions on the DIR. Three boundary conditions including clamped-clamped (CC), clamped-simply (CS) and simply-simply (SS) are considered. It is concluded that the DIR of the beam with CC boundary condition is happened at higher excitation frequency with respect to the beam with SS and CS boundary conditions. It is since, the beam with CC boundary condition has higher bending rigidity.

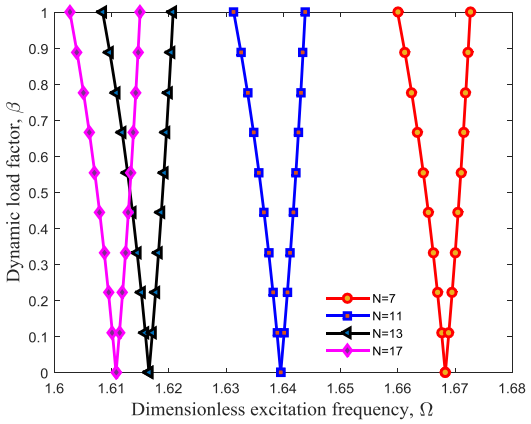

Fig. 2 The convergence of the proposed method

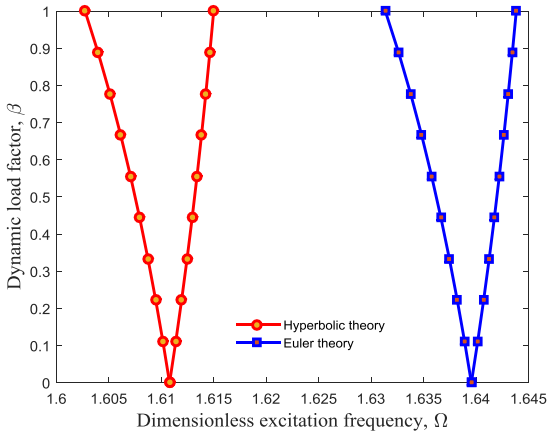

Fig. 3 Comparison the results predicted by hyperbolic and Euler theories

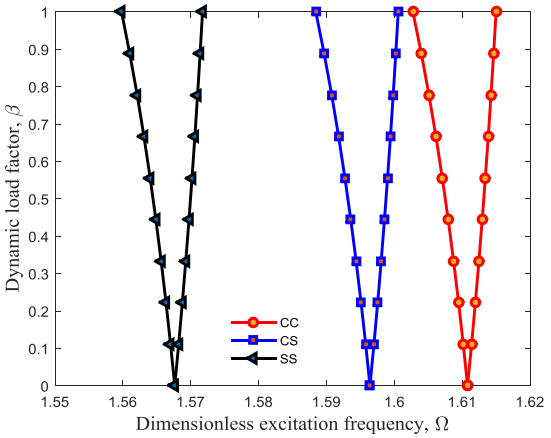

Fig. 4 The effect of different boundary condition on the DIR of the structure

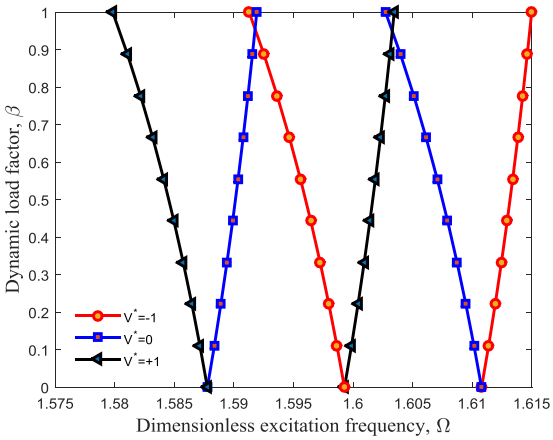

Fig. 5 The effect of the applied electric voltage on the DIR of the structure

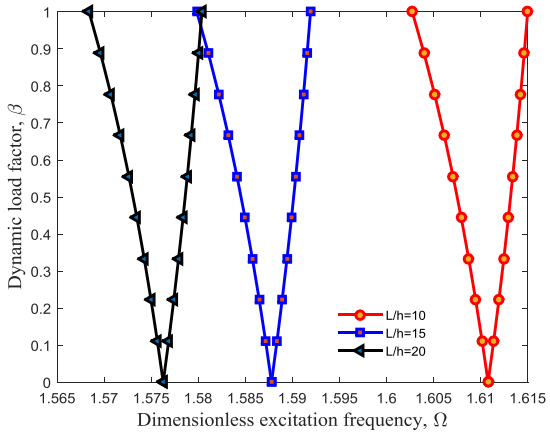

Fig. 6 The effect of length to the total thickness ratio on the DIR of the structure

The influence of the non-dimensional applied electric voltage ($V^* = (V_0 / h_t)\sqrt{E_c / \in_{11}}$) on the DIR of the sandwich structure is shown in Fig. 5. It can be found that with applying the positive voltage, the DIR shifts to lower excitation frequency. This is because of the generation of the tensile and compressive forces resulting of the positive and negative voltage applied to the piezoelectric layer (i.e., actuator), respectively.

The effect of length to the total thickness ratio of the structure on the DIR is shown in Figs. 6. As can be seen with raising the length to the total thickness ratio of the structure, the DIR shifts to lower excitation frequency. It is because with raising the length to the total thickness ratio of the structure, the stiffness reduces.

Fig. 7 depicts the influence of the top to core thickness ratio on the DIR of the sandwich structure. It can be concluded that with increasing the top to core thickness ratio, the DIR will be happened at higher excitation frequencies. The reason is that with increasing the top to core thickness ratio, the stiffness of the structure improves.

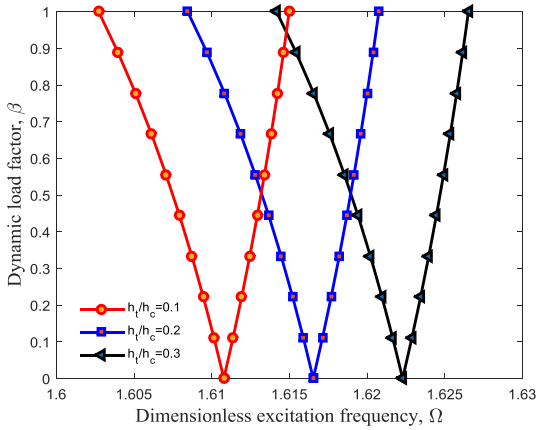

Fig. 7 The effect top to core thickness ratio on the DIR of the structure

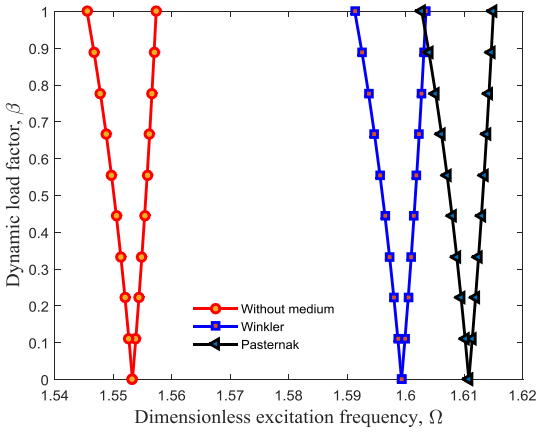

Fig. 8 The effect of the elastic foundation on the DIR of the structure

Fig. 8 demonstrates the influence of different types of elastic mediums on the DIR the structure. As can be seen, considering the elastic medium causes to increase in the excitation frequency of the structure. The reason is that the existence of the elastic medium makes the system stiffer. Furthermore, it can be concluded that the DIR for Pasternak medium will be happened at higher excitation frequencies with respect to Winkler ones. It is because the stiffness of the structure with Pasternak foundation is higher than Winkler cases.

5. Conclusions

Dynamic buckling of smart sandwich beam was presented in this work based on hyperbolic theory. The structure was located in elastic foundation with spring and shear elements. Based on energy method and Hamilton's principle, the motion equations were derived. DQ-Bolotin methods were applied for obtaining the DIR of the structure. The effects of applied voltage, geometrical parameters of structure and boundary conditions on the DIR

of the structure were shown. The results show that the DIR of the beam with CC boundary condition was happened at higher excitation frequency with respect to the beam with SS and CS boundary conditions. It can be found that with applying the positive voltage, the DIR shifts to lower excitation frequency. In addition, with raising the length to the total thickness ratio of the structure, the DIR shifts to lower excitation frequency. Furthermore, with increasing the top to core thickness ratio, the DIR will be happened at higher excitation frequencies. Meanwhile, the DIR for Pasternak medium will be happened at higher excitation frequencies with respect to Winkler ones.

References

Attia, A., Tounsi, A., Adda Bedia, E.A. and Mahmoud, S.R. (2015), "Free vibration analysis of functionally graded plates with temperature-dependent properties using various four variable refined plate theories", *Steel Compos. Struct*., **18**(1), 187-212.

Cafarova, F.I., Akbarov, S.D. and Yahnioglu, N. (2017), "Buckling delamination of the PZT/Metal/PZT sandwich circular plate-disc with penny-shaped interface cracks", *Smart Struct. Syst*., **19**(2), 163-179.

Chai, Y.Y., Song, Zh.G. and Li, F.M. (2017), "Investigations on the influences of elastic foundations on the aerothermoelastic flutter and thermal buckling properties of lattice sandwich panels in supersonic airflow", *Acta Astronautic.*, **140**, 176-189.

Draiche, K., Tounsi, A. and Mahmoud, S.R. (2016), "A refined theory with stretching effect for the flexure analysis of laminated composite plates", *Geomech. Eng.*, **11**(5), 671-690.

Duc, N.D., Cong, P.H., Tuan, N.D., Tran, P. and Van Thanh, N. (2017a), "Thermal and mechanical stability of functionally graded carbon nanotubes (FG CNT)-reinforced composite truncated conical shells surrounded by the elastic foundation", *Thin-Wall. Struct*., **115**, 300-310.

Duc, N.D., Hadavinia, H., Van Thu, P. and Quan, T.Q. (2015), "Vibration and nonlinear dynamic response of imperfect three-phase polymer nanocomposite panel resting on elastic foundations under hydrodynamic loads", *Compos. Struct*., **131**, 229-237.

Duc, N.D., Lee, J., Nguyen-Thoi, T. and Thang, P.T. (2017b), "Static response and free vibration of functionally graded carbon nanotube-reinforced composite rectangular plates resting on Winkler–Pasternak elastic foundations", *Aerosp. Sci. Technol*., **68**, 391-402.

Duc, N.D., Seung-Eock, K., Quan, T.Q., Long, D.D. and Anh, V.M. (2018), "Nonlinear dynamic response and vibration of nanocomposite multilayer organic solar cell", *Compos. Struct*., **184**, 1137-1144.

Duc, N.D., Tran, Q.Q. and Nguyen, D.K. (2017c), "New approach to investigate nonlinear dynamic response and vibration of imperfect functionally graded carbon nanotube reinforced composite double curved shallow shells subjected to blast load and temperature", *Aerosp. Sci. Technol*., **71**, 360-372.

Ghini, Y. and Vacca, A. (2018), "A method to perform prognostics in electro-hydraulic machines: the case of an independent metering controlled hydraulic crane", *Int. J. Hydromechatronics*, **1**, 197-221.

Henderson, J.P., Plummer, A. and Johnston, N. (2018), "An electro-hydrostatic actuator for hybrid active-passive vibration isolation", *Int. J. Hydromechatronics*, **1**, 47-71.

Katariya, P.V., Panda, S.K., Hirwani, Ch.K., Mehar, K. and Thakare, O. (2017), "Enhancement of thermal buckling strength of laminated sandwich composite panel structure embedded with shape memory alloy fibre", *Smart Struct. Syst*., **20**(5), 595-605.

Khetir, H., Bouiadjra, M.B., Houari, M.S.A., Tounsi, A. and Mahmoud, S.R. (2017), "A new nonlocal trigonometric shear deformation theory for thermal buckling analysis of embedded nanosize FG plates", *Struct. Eng. Mech*., **64**(4), 391-402.

Larbi Chaht, F., Kaci, A., Houari, M.S.A. and Hassan, S. (2015), "Bending and buckling analyses of functionally graded material (FGM) size-dependent nanoscale beams including the thickness stretching effect" *Steel Compos. Struct.*, **18**(2), 425 -442.

Latifi, M., Kharazi, M. and Ovesy, H.R. (2018), "Nonlinear dynamic instability analysis of sandwich beams with integral viscoelastic core using different criteria", *Compos. Struct.*, **191**, 89-99.

Li, X., Yu, K. and Zhao, R. (2018), "Thermal post-buckling and vibration analysis of a symmetric sandwich beam with clamped and simply supported boundary conditions", *Arch. Appl. Mech*., **88**, 543-561.

Madani, H., Hosseini, H. and Shokravi, M. (2016), "Differential cubature method for vibration analysis of embedded FG-CNT-reinforced piezoelectric cylindrical shells subjected to uniform and non-uniform temperature distributions", *Steel Compos. Struct*., **22**, 889-913.

Mahi, A., Bedia, E.A.A. and Tounsi, A. (2015), "A new hyperbolic shear deformation theory for bending and free vibration analysis of isotropic, functionally graded, sandwich and laminated composite plates", *Appl. Math. Model*., **39**, 2489-2508.

Mehri, M., Asadi, H. and Wang, Q. (2016), "Buckling and vibration analysis of a pressurized CNT reinforced functionally graded truncated conical shell under an axial compression using HDQ method", *Comput. Method. Appl. M.*, **303**, 75-100.

Menasria, A., Bouhadra, A., Tounsi, A. and Hassan, S. (2017), "A new and simple HSDT for thermal stability analysis of FG sandwich plates", *Steel Compos. Struct*., **25**(2), 157-175.

Meziane, M.A.A., Abdelaziz, H.H. and Tounsi, A.T. (2014), "An efficient and simple refined theory for buckling and free vibration of exponentially graded sandwich plates under various boundary conditions", *J. Sandw. Struct. Mater*., **16**(3), 293-318.

Mouffoki, A., Adda Bedia, E.A., Houari M.S.A. and Hassan, S. (2017), "Vibration analysis of nonlocal advanced nanobeams in hygro-thermal environment using a new two-unknown trigonometric shear deformation beam theory", *Smart Struct. Syst*., **20**(3), 369-383.

Sayyad, A.S. and Ghugal, Y.M. (2017), "Bending, buckling and free vibration of laminated composite and sandwich beams: A critical review of literature", *Compos. Struct.*, **171**, 486-504.

Shamshuddin Sayyad, A. and Ghugal, Y.M. (2018), "Effect of thickness stretching on the static deformations, natural frequencies, and critical buckling loads of laminated composite and sandwich beams", *J. Braz. Soc. Mech. Sci. Eng*., **40**, 296-302.

Shokravi, M. (2017a), "Buckling of sandwich plates with FG-CNT-reinforced layers resting on orthotropic elastic medium using Reddy plate theory", *Steel Compos. Struct*., **23**(6), 623-631.

Shokravi, M. (2017b), "Buckling analysis of embedded laminated plates with agglomerated CNT-reinforced composite layers using FSDT and DQM", *Geomech. Eng*., **12**, 327-346.

Shokravi, M. (2017c), "Vibration analysis of silica nanoparticles-reinforced concrete beams considering agglomeration effects", *Comput. Concrete*, **19**, 333-338.

Shokravi, M. and Jalili, N. (2017), "Dynamic buckling response of temperature-dependent functionally graded-carbon nanotubes-reinforced sandwich microplates considering structural damping", *Smart Struct. Syst*., **20**(5), 583-593.

Simsek, M. and Reddy, J.N. (2013), "A unified higher order beam

theory for buckling of a functionally graded microbeam embedded in elastic medium using modified couple stress theory", *Compos. Struct*., **101**, 47-58.

Song, Zh.G. and Li, F.M. (2018), "Flutter and buckling characteristics and active control of sandwich panels with triangular lattice core in supersonic airflow", *Compos. Part B: Eng.*, **108**, 334-344.

Thanh, N.V., Khoa, N.D., Tuan, N.D., Tran, P. and Duc, N.D. (2017), "Nonlinear dynamic response and vibration of functionally graded carbon nanotube-reinforced composite (FG-CNTRC) shear deformable plates with temperature-dependent material properties", *J. Therm. Stres.*, **40**, 1254-1274.

Trinh, M.Ch. and Kim, S.E. (2018), "Nonlinear thermomechanical behaviors of thin functionally graded sandwich shells with double curvature", *Compos. Struct.*, **195**, 335-348.

Van Do, V.N. and Lee, Ch.H. (2017), "Thermal buckling analyses of FGM sandwich plates using the improved radial point interpolation mesh-free method", *Compos. Struct.*, **177**, 171-186.

Van Thu, P. and Duc, N.D. (2016), "Non-linear dynamic response and vibration of an imperfect three-phase laminated nanocomposite cylindrical panel resting on elastic foundations in thermal environment", *Sci. Eng. Compos. Mat*., **24** (6), 951-962.

Yang, H. and Yu, L. (2017), "Feature extraction of wood-hole defects using wavelet-based ultrasonic testing", *J. Forest. Res.*, **28**, 395-402

Ying, Z.G., Ni, Y.Q. and Duan, Y.F. (2017), "Stochastic vibration suppression analysis of an optimal bounded controlled sandwich beam with MR visco-elastomer core", *Smart Struct. Syst.*, **19**(1), 21-31.

CC